

Sequential and simultaneous emission of fragments from p+Al collisions

M.Fidelus,¹ D.Filges,^{2,3} F.Goldenbaum,^{2,3} H.Hodde,⁴ A.Jany,¹ L.Jarczyk,¹ B.Kamys,^{1,*}
M.Kistryn,⁵ St.Kistryn,¹ St.Kliczewski,⁵ E.Kozik,⁵ P.Kulesa,⁵ H.Machner,⁶ A.Magiera,¹
B.Piskor-Ignatowicz,^{1,2,3} K.Pysz,⁵ Z.Rudy,¹ Sushil K. Sharma,^{1,2,3} R.Siudak,⁵ and M.Wojciechowski¹
(PISA - Proton Induced SpAlliation collaboration)

¹*M. Smoluchowski Institute of Physics, Jagiellonian University, Reymonta 4, 30059 Kraków, Poland*

²*Jülich Center for Hadron Physics, Forschungszentrum Jülich, 52425 Jülich, Germany*

³*Institut für Kernphysik, Forschungszentrum Jülich, 52425 Jülich, Germany*

⁴*Institut für Strahlen- und Kernphysik, Bonn University, 53121 Bonn, Germany*

⁵*H. Niewodniczański Institute of Nuclear Physics PAN, Radzikowskiego 152, 31342 Kraków, Poland*

⁶*Universität Duisburg-Essen, Fakultät für Physik, Lotharstr.1, 47048 Duisburg, Germany*

(Dated: June 6, 2022)

The energy and angular dependence of double differential cross sections $d^2\sigma/d\Omega dE$ were measured for $p, d, t, {}^3,4,6\text{He}, {}^6,7,8\text{Li}, {}^7,9,10\text{Be}$, and ${}^{10,11,12}\text{B}$ produced in collisions of 1.2, 1.9, and 2.5 GeV protons with an Al target. The spectra and angular distributions of Li, Be, and B isotopes indicate a presence of two contributions: an isotropic, low energy one which is attributed to the evaporation of particles from excited remnants of the intranuclear cascade, and an anisotropic part which is interpreted to be due to multifragmentation of the remnants. It was found that such a hypothesis leads to a very good description of spectra and angular distributions of all intermediate mass fragments (${}^6\text{He}$ - ${}^{12}\text{B}$) using the critical value of the excitation energy per nucleon as a single parameter, varying slowly with the beam energy.

PACS numbers: 25.40.-h, 25.40.Sc, 25.40.Ve

Keywords: Proton induced reactions, production of intermediate mass fragments, multifragmentation, critical excitation energy

I. INTRODUCTION

In recent studies of reactions induced by GeV protons on Au [1, 2] and Ni targets [3, 4], it has been found that the inclusive spectra of intermediate mass fragments (IMF), *i.e.*, particles with $Z \geq 3$, but lighter than fission fragments, as *e.g.* Li, Be, B, etc., contain two components which differ in energy and angular dependencies. The low energy component of the spectra is almost angle independent, while the high energy part of the spectra changes with the angle becoming more steep with increasing scattering angle. These properties of the spectra could not be quantitatively reproduced by the traditional two step model which assumes that the first stage of the reaction proceeds via an intranuclear cascade of the nucleon-nucleon and nucleon-pion collisions leaving the excited target remnant in equilibrium whereas the second stage consists in the evaporation of nucleons and composite particles.

The same effect of the presence of two components in the spectra has been observed for various target nuclei by other authors, *e.g.*, by Green *et al.* [5, 6] for reactions in p+Ag system at $T_p=0.21, 0.3$, and 0.48 GeV, by Herbach *et al.* [7] for target nuclei between Al and Th at 1.2 GeV, by Letourneau *et al.* [8] for p+Au collisions at 2.5 GeV, by Westfall *et al.* [9] for C, Al, Ag and U targets irradiated by protons of 2.1 and 4.9 GeV energies, by

Hyde *et al.* [10] for p+Ag system at 5.5 GeV, and by Poskanzer *et al.* [11] for p+U reactions at 5.5 GeV.

The analysis of the energy and angular dependencies of differential cross sections for IMFs from p+Au and p+Ni reactions [1–4] has shown that the data can be well reproduced by a phenomenological model which assumes that the composite particles are emitted isotropically from two sources moving along the beam direction. The break-up of bombarded nuclei, occurring in the first stage of the collision, was proposed [1] to account for the observed phenomenon.

The competitive hypothesis, which is studied in the present work, states that the excited nuclei are divided into two groups not due to the geometrical conditions imposed by their creation mode but on the contrary, by their decay. It may be conjectured that the decay mode of the excited nuclei depends mainly on their excitation energy per nucleon. The nuclei which have small excitation energy evaporate nucleons and composite particles, whereas the highly excited nuclei (above some critical energy per nucleon) may undergo a phase transition, *i.e.* multifragmentation appears [12, 13]. The energy available in the multifragmentation is usually larger than that in the evaporation process because the multifragmentation appears only for highly excited nuclei. Furthermore, the full excitation energy is then released in a single act, whereas the evaporation consists of several steps in which light particles take a part of the excitation energy and heavy residues of the evaporation have smaller energy – due to the momentum conservation in each consecutive two-body decay of the de-exciting nucleus. Thus, the

*Corresponding author: ufkamys@cyf-kr.edu.pl

intermediate mass fragments emitted from a multifragmentation could have on average larger energies than the evaporation residua with the same mass. Due to this fact, the evaporation should give rise to qualitatively different spectra than emission of the same heavy particles in the multifragmentation. This effect can explain the appearance of two qualitatively different components of the spectra of intermediate mass fragments. Thus, the present study concentrates on the investigation of the discussed above hypothesis concerning properties of the spectra of intermediate mass fragments.

Since exact calculations of multifragmentation of heavy nuclei are practically not possible due to an enormous number of involved partitions, and since the intranuclear cascade models, which neglect the shell structure of nuclei might not work well for very light nuclei (cf., *e.g.*, Z. Fraenkel *et al.* [14]), the choice of the target nucleus for investigation of validity of the above proposed hypothesis should fulfill a compromise between these two constraints. The aluminium target has been therefore selected for the present study.

The paper is organized as follows: the experimental details are discussed in the next section, the analysis of the IMF data performed by means of the intranuclear cascade (for the first stage of the reaction) combined with evaporation and multifragmentation (for the second step) is presented in the third section, and the last section summarizes the obtained results.

II. EXPERIMENTAL RESULTS

The PISA experiment has been performed using the internal beam of COSY (COoler SYnchrotron) of the Research Center in Juelich. The apparatus and experimental procedure have been described in previous publications [1, 2, 4] thus in the present work only details, characteristic for the studied reactions are discussed.

Self-supporting aluminium target of the $170 \mu\text{g}/\text{cm}^2$ thickness was bombarded by the internal proton beam of COSY. Three beam energies were used: 1.2, 1.9, and 2.5 GeV. To assure the same experimental conditions for all beam energies COSY operated in the so called supercycle mode. In this mode several cycles were alternated for each requested beam energy, consisting of protons injection from the cyclotron JULIC to COSY ring, their acceleration with the beam circulating in the ring below the target, and irradiating the target by slow movement of the beam in the upward direction. Due to the application of the supercycle mode of the target irradiation all conditions of the experiment except the energy of the proton beam remained unchanged. This allowed to minimize the effect of systematic uncertainties on the energy dependence of the measured cross sections.

Double differential cross sections $d^2\sigma/d\Omega dE$ were measured at seven scattering angles: 15.6° , 20° , 35° , 50° , 65° , 80° , and 100° . The mass and charge identification of detected particles was realized by the $\Delta E - E$ method

using telescopes consisted of silicon semiconductor detectors backed (in four cases: 15.6° , 20° , 65° , and 100°) by a 7 cm thick CsI detector with a photo-diode readout, which were used to detect high energy light charged particles passing through the silicon detectors.

The $d^2\sigma/d\Omega dE$ were measured for the following ejectiles: p, d, t, $^3,4,6\text{He}$, $^6,7,8,9\text{Li}$, $^7,9,10\text{Be}$, $^{10,11,12}\text{B}$ and C. Here we will concentrate on the IMF data. Discussion on the light charged particle emission will be published separately.

In order to allow for absolute normalization of differential cross sections we performed a "two moving sources" fit to $d^2\sigma/d\Omega dE$ for ^7Be production in our experiment and compared the resulting total cross section with data from ref. [15]. It was found that the angular and energy dependence of $d^2\sigma/d\Omega dE$ can be well reproduced by a simple formula representing the isotropic emission from two sources moving forward along the beam direction. Each source emitting particles with Maxwellian energy distribution was characterized by its velocity β , temperature T , height of the Coulomb barrier between ^7Be and the source remnant described by parameter k , and by emission intensity σ (see Appendix of ref. [1] for details of the parametrization). The σ parameter has the meaning of the energy and angle integrated cross section attributed to a given source. Thus, the not normalized cross section $\sigma_{a.u.}$ for ^7Be production is equal to the sum of parameters $\sigma_1 + \sigma_2$ for both sources. Best values of the parameters were found by fitting simultaneously the full set of the ^7Be spectra (seven scattering angles). Alas, the fits lead to ambiguous results because the experimental spectra did not cover the full energy range allowed by kinematics. Low energy particles were not registered because of finite low-energy detection thresholds of the telescopes. This lack of information on the low energy part of spectra could strongly influence the value of the energy integrated cross section since the spectra have Maxwellian shape with its maximum lying in the neighborhood of the energy threshold. Fortunately, it turned out that the spread of values of σ parameters was smaller than 10 % among the sets of parameters which provided the same, best χ^2 values obtained for various combinations of fixed Coulomb barrier parameters k_1 and k_2 . The final values of the σ parameters for both sources were taken as the arithmetic mean of results obtained for equivalent quality fits, *i.e.*, those which have the same, smallest χ^2 value. The error of the normalization factor obtained in such a way was $\approx 9\%$ for all studied energies. This value does not include the inaccuracy of the literature value of the production cross section $\sigma(^7\text{Be})$ [15] which is believed to be smaller than 10%.

The good quality of the absolute normalization of the present experiment is confirmed by a comparison of the obtained differential cross sections with the data from literature. To our knowledge only one measurement of light charged particle spectra as well as intermediate mass fragment spectra is present in the literature for aluminium target at proton beam energies similar to those

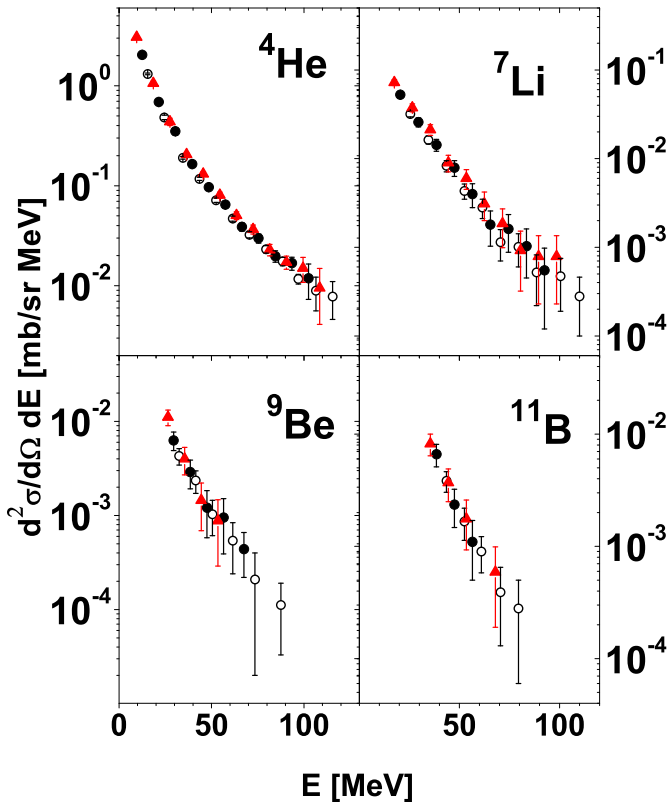


FIG. 1: Spectra of ${}^4\text{He}$, ${}^7\text{Li}$, ${}^9\text{Be}$, ${}^{11}\text{B}$ measured at 35° for p+Al collisions at three proton beam energies: 1.2 (circles), 1.9 (full circles), and 2.5 GeV (triangles). To avoid overlapping of symbols only different energy bins are shown for different beam energies.

used in the present study. This is the paper of Westfall *et al.* [9] dealing with reactions in the p+Al system investigated at 4.9 GeV proton energy. This energy is 2–4 times higher than those used in the present work, however, it is known that the total production cross sections for this target vary only slightly at proton beam energies larger than 1 GeV (cf. *e.g.* ref. [15]). The differential cross sections measured in the present experiment also change only slightly with the beam energy as it is shown in Fig. 1. As can be seen, the cross sections increase very slightly with the increasing beam energy. This increase is stronger for lighter ejectiles (${}^4\text{He}$, ${}^7\text{Li}$), whereas the data for heavier IMFs are in the limits of errors independent of the beam energy.

The weak energy dependence of the differential cross sections leads to the conclusion, that it is reasonable to compare the present data with results obtained by Westfall *et al.* [9] at even higher incident proton energy. Such a comparison is depicted in Fig. 2 for lithium, beryllium and boron isotopes. As can be seen, the shapes and magnitudes of the spectra are in excellent agreement for all ejectiles.

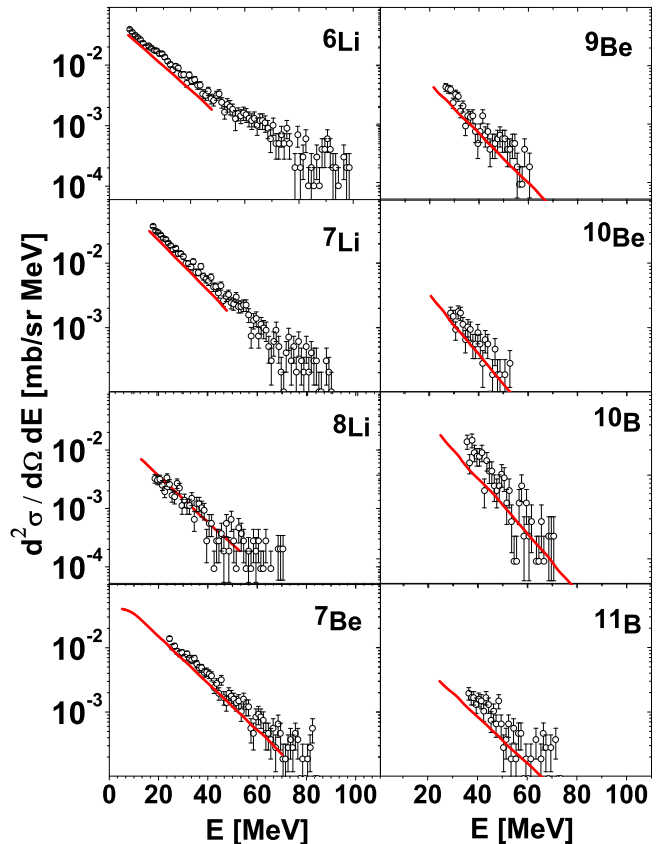


FIG. 2: Experimental spectra of Li, Be, and B from the present work (circles) measured at 100° in p+Al collisions at proton beam energy 2.5 GeV and data from ref. [9] measured at 90° at proton energy 4.9 GeV (lines).

III. THEORETICAL ANALYSIS

The model calculations of the first stage of the reaction were done by means of the INCL4.3 computer program [16, 17] realizing the intranuclear cascade of nucleon-nucleon collisions. The decay of remnant nuclei (A, Z) excited to the energy E^* was evaluated in the frame of two different models: the generalized evaporation model GEM2 of S. Furihata [18, 19] and the multifragmentation treated as the Fermi breakup model using the computer program ROZPAD of A. Magiera [20].

The Fermi breakup model [21–23] assumes that the probability W of disintegration of an excited nucleus with mass M and volume V into channel containing n fragments with masses m_i and spins s_i ($i = 1, 2, \dots, n$) is proportional to its phase space volume [23]

$$W \sim \frac{g}{G} \left[\frac{V}{(2\pi\hbar)^3} \right]^{n-1} \left(\frac{1}{M} \prod_{i=1}^n m_i \right)^{3/2} \frac{(2\pi)^{3(n-1)/2}}{\Gamma\left(\frac{3(n-1)}{2}\right)} E_{kin}^{(3n-5)/2}$$

where g is the number of spin projections of n fragments

$g = \prod_{i=1}^n (2s_i + 1)$, $G = 1 / \prod_{j=1}^k n_j!$ accounts for identity of

n_j fragments of kind j (k is defined by $n = \sum_{j=1}^k n_j$), and

$\Gamma(x)$ is the gamma function. The total kinetic energy of n fragments at the moment of breakup E_{kin} is related to the excitation energy E^* of the decaying nucleus (A, Z) according to the equation:

$$E_{kin} = (E^* + Mc^2) - \sum_{i=1}^n m_i c^2 - U_n^C$$

where U_n^C represents the Coulomb interaction energy of the fragments.

The double differential cross sections $d^2\sigma/d\Omega dE$ are obtained in the Fermi breakup model by random generation of energies and flight directions of fragments over the whole accessible phase space [23].

It should be pointed out that the Fermi breakup model gives statistical method of dealing with the multifragmentation process based on the assumption of full equilibration of the excited system in which the energy and linear momentum conservation is exactly taken into account. In the following the "multifragmentation" will be understood as such a specific model of this process.

It was assumed that the sequential emission of IMFs, *i.e.*, the evaporation of a single particle in each step, dominates when the remnants of the cascade are excited to low energies whereas the remnants with higher excitation energies split simultaneously into many pieces thus they are subject of multifragmentation. *The critical excitation energy per nucleon $(E^*/A)_{cr}$* , *i.e.*, the smallest value of excitation energy per nucleon at which multifragmentation appears was treated in the present work as a free parameter. The only free parameter of the Fermi breakup model - the so called *freeze-out radius r_0* was also fitted. It has the meaning of a reduced radius of the decaying, spherical nucleus of the mass number A , *i.e.* the volume V of the decaying nucleus is calculated as $V = 4\pi r_0^3 A/3$. The default value of the r_0 parameter used in the GEANT4 is equal to 1.4 fm [23].

The free parameters of the present model: freeze-out radius r_0 and critical excitation energy $(E^*/A)_{cr}$ were searched for by comparison of theoretical spectra with the experimental data, for ${}^6\text{He}$, ${}^{6,7,8,9}\text{Li}$, ${}^{7,9,10}\text{Be}$, and ${}^{10,11,12}\text{B}$. Chi-square values χ^2 were evaluated summing over all these data, *i.e.* over all ejectiles listed above and over seven scattering angles for each of these ejectiles for several fixed values of r_0 parameter and several values of critical excitation energy $(E^*/A)_{cr}$. The obtained values of the chi-square are shown in Fig. 3 for proton beam energy 1.2 GeV.

The following properties of the chi-square dependence are clearly visible:

- Broad minima of the chi-square treated as a function of the critical excitation energy $(E^*/A)_{cr}$ are present for each fixed value of the r_0 parameter. The chi-square increases very strongly when

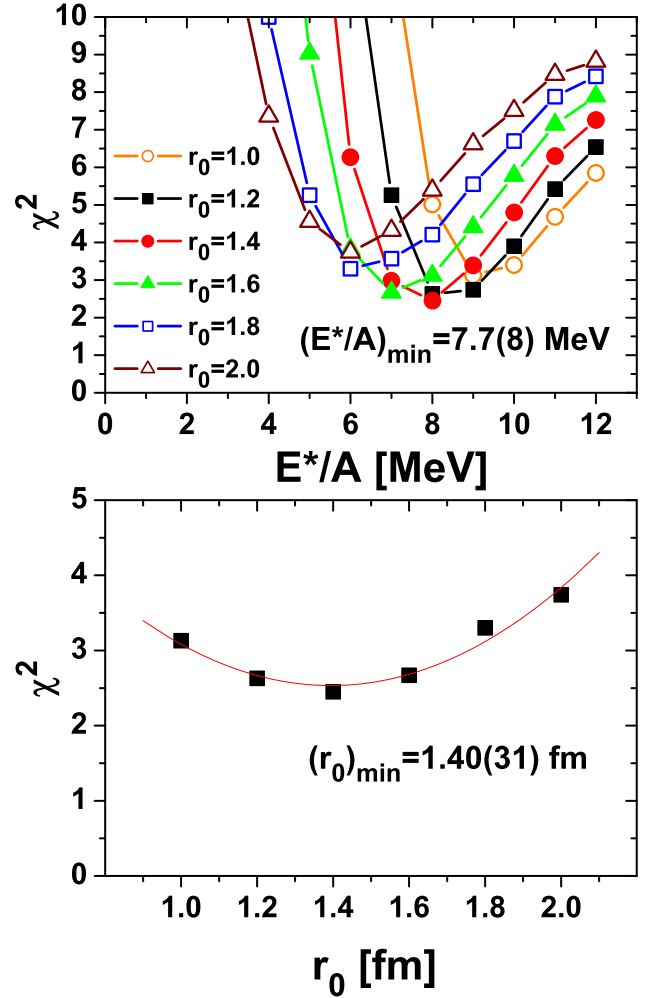


FIG. 3: Results of the analysis for the proton beam energy equal to 1.2 GeV. Upper panel: chi-square values versus critical value of the excitation energy per nucleon $(E^*/A)_{cr}$ for several values of reduced freeze-out radius r_0 (in fm). Lower panel: Minimal values of the chi-square for each value of r_0 .

the critical excitation energy decreases to values smaller than ≈ 5 MeV/nucleon. This behavior points to the fact that the nuclei at such low excitation energies are not subject of the multifragmentation but rather sequentially evaporate particles.

- Minimal value of the chi-square for each value of the r_0 parameter, found from the chi-square dependence on $(E^*/A)_{cr}$, is presented as a function of r_0 in the lower panel of the Fig. 3. As can be seen, this dependence may be well approximated by a concave parabolic function, which minimum allows to choose the best fit value of the r_0 parameter.

The fit procedure described above has been applied to the data measured at all three proton beam energies: 1.2, 1.9, and 2.5 GeV, leading to the same (in the limits of errors) best fit values for the reduced radius r_0 : 1.40(31)

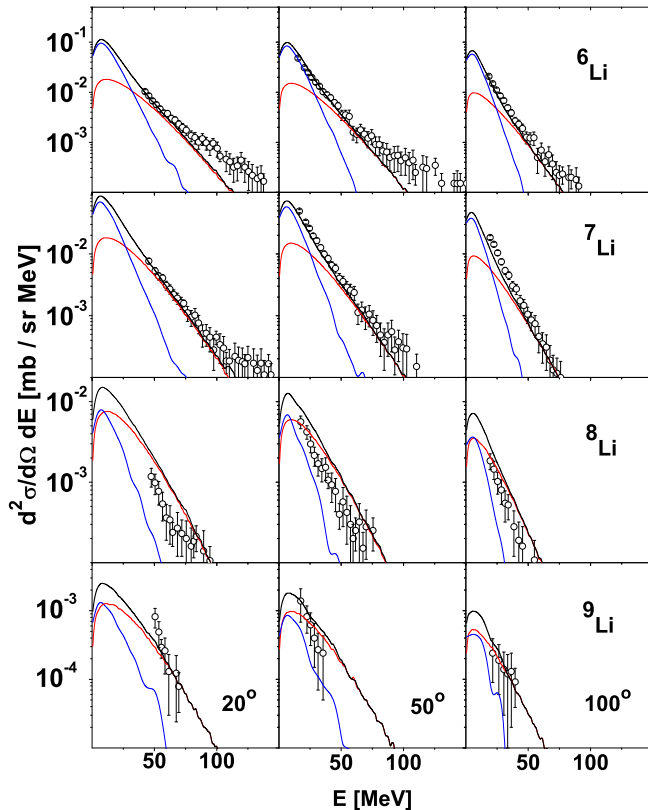


FIG. 4: Experimental spectra (circles) measured at three scattering angles: 20° , 50° , and 100° (left, middle, and right columns) for ${}^6\text{Li}$, ${}^7\text{Li}$, ${}^8\text{Li}$, and ${}^9\text{Li}$ (upper, middle, and lower rows) for p+Al collisions at proton beam energy of 1.2 GeV. The lines represent theoretical calculations: blue (the steepest), red (the least steep), and black lines correspond to evaporation, multifragmentation, and their sum, respectively.

fm, 1.40(25) fm, and 1.39(43) fm for beam energy 1.2, 1.9, and 2.5 GeV, respectively. It is worth pointing out that the obtained values of r_0 parameter are equal in the limits of errors to $r_0 = 1.4$ fm assumed as the default value in the literature [23]. Thus fixing the parameter r_0 at $r_0 = 1.40(20)$ fm allows to find the best fit value of the second parameter - the critical excitation energy $(E^*/A)_{cr}$ - independently for each beam energy.

It was found that the critical excitation energy is also almost the same in the studied beam energy range. It is equal to 7.7(8) MeV/nucleon, 7.0(8) MeV/nucleon, and 6.1(9) MeV/nucleon for 1.2, 1.9, and 2.5 GeV beam energy, respectively.

The quality of the description of experimental data for p+Al collisions may be judged from inspection of Figs 4 - 6, where a representative sample of the data measured at proton beam energy equal to 1.2 GeV is shown. As can be seen, the contribution of multifragmentation to the spectra (shown by the least-steep, red line in the figures) is crucial for reproducing high energy parts of the spectra of IMFs. On the other hand the evaporation

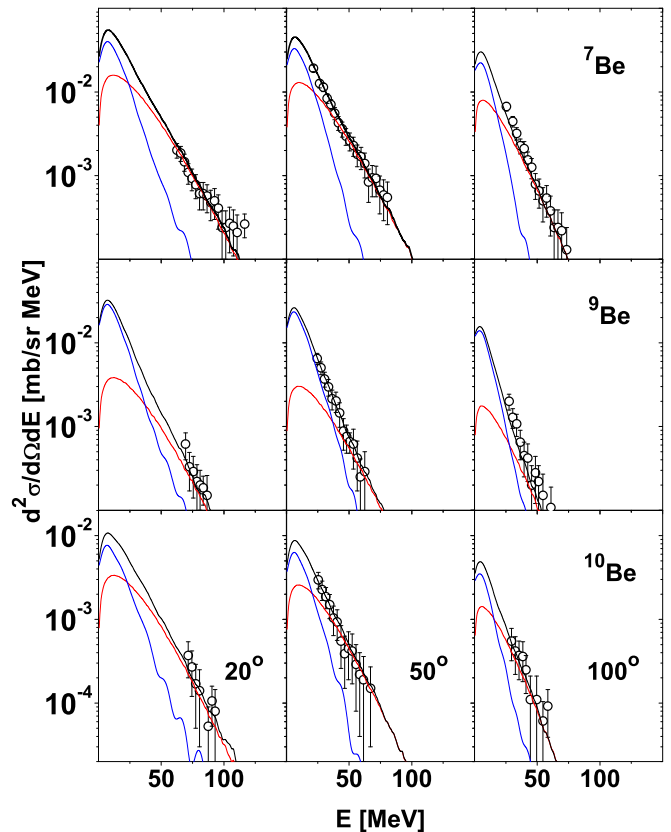


FIG. 5: Same as in Fig. 4 but for ${}^7\text{Be}$, ${}^9\text{Be}$, and ${}^{10}\text{Be}$, respectively

which leads to very steep shape of the spectra is not able to describe their high energy tails but dominates at low energies of the ejectiles. It turned out that the sum of evaporation and multifragmentation describes very well the full spectra of ${}^6,7,8,9\text{Li}$, ${}^7,9,10\text{Be}$, and ${}^{10,11,12}\text{B}$. Note that the fluctuations of the theoretical curves visible in the figures have no meaning - they are only due to a limited statistics of the Monte Carlo calculations.

It should be emphasized that all the spectra shown here, obtained at 1.2 GeV proton beam energy, are reproduced assuming the same values of the parameters: $r_0 = 1.4$ fm and $(E^*/A)_{cr} = 7.7$ MeV.

An equally good description of IMF data was achieved for higher beam energies (1.9 and 2.5 GeV) using the same value of r_0 parameter and appropriate critical excitation energies. Since the shape of the spectra almost does not change with the beam energy, the Figs 4 - 6 are representative for the quality of data reproduction obtained at all studied energies.

The angle and energy integrated double differential cross sections $d^2\sigma/d\Omega dE$ obtained in the analysis described above are collected in Table I. The following conclusions can be derived:

- Evaporation cross sections decrease quickly with beam energy for all IMFs, on the contrary to

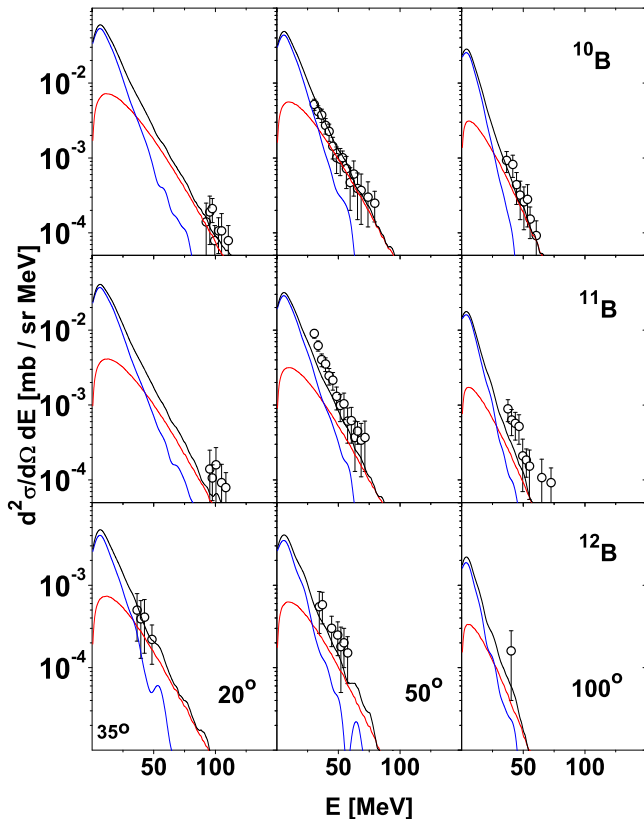


FIG. 6: Same as in Fig. 4 but for ^{10}B , ^{11}B , and ^{12}B , respectively

increasing of multifragmentation cross sections. These monotonic dependencies lead to the fast increase of the relative contribution of multifragmentation to the total cross section.

- The multifragmentation contribution dominates for all ejectiles at the highest beam energy. It exhausts at least 51% of the total cross section (for ^{11}B) but for a few ejectiles it reaches even 95% (for ^8Li and ^9Li).
- The sum of both contributions increases with the beam energy but not as quickly as the fragmentation cross sections themselves because of decreasing of the evaporation contribution. The ratio of the total production cross section at the beam energy of 2.5 GeV to that at 1.2 GeV varies from about 1.1 for ^6Li and ^{11}B to about 2.2 for ^9Li .

It was checked whether the parameter of the present model, *i.e.* the critical excitation energy per nucleon $(E^*/A)_{cr}$ is compatible with the critical excitation energy found from the analysis of the caloric curves. For this purpose the values of the critical energy obtained in the present investigation were compared with those from a compilation of caloric curve results published by Natovitz *et al.* [24]. The target mass dependence of the

TABLE I: Total production cross sections of intermediate mass fragments for p+Al collisions at three proton beam energies: 1.2, 1.9, and 2.5 GeV. In the first column the symbol of the ejectile is listed, in the second column the beam energy is specified, and in the following columns the production cross section due to the sequential evaporation, production cross section due to the multifragmentation, the sum of both cross sections, and the relative contribution of the multifragmentation to the total cross section are presented.

particle	energy [GeV]	σ_{GEM} [mb]	σ_{FBM} [mb]	σ_{Tot} [mb]	σ_{FBM} [%]
^6He	1.2	0.57	1.03	1.60	64
	1.9	0.45	1.68	2.13	79
	2.5	0.34	2.33	2.67	87
^6Li	1.2	9.81	4.28	14.09	30
	1.9	7.35	7.02	14.37	49
	2.5	5.60	9.32	14.92	62
^7Li	1.2	3.57	4.04	7.61	53
	1.9	2.72	6.61	9.33	71
	2.5	1.95	9.40	11.35	83
^8Li	1.2	0.37	1.55	1.92	81
	1.9	0.28	2.55	2.83	90
	2.5	0.21	3.71	3.92	95
^9Li	1.2	0.056	0.24	0.296	81
	1.9	0.046	0.42	0.466	90
	2.5	0.033	0.62	0.653	95
^7Be	1.2	2.19	3.56	5.75	62
	1.9	1.66	6.17	7.83	79
	2.5	1.24	7.98	9.22	87
^9Be	1.2	1.63	0.78	2.41	32
	1.9	1.30	1.37	2.67	51
	2.5	0.99	2.20	3.19	69
^{10}Be	1.2	0.78	0.64	1.42	45
	1.9	0.63	1.13	1.76	64
	2.5	0.45	1.91	2.36	81
^{10}B	1.2	5.86	1.39	7.25	19
	1.9	4.81	2.65	7.46	36
	2.5	3.73	4.23	7.96	53
^{11}B	1.2	4.36	0.77	5.13	15
	1.9	3.52	1.50	5.02	30
	2.5	2.57	2.71	5.28	51
^{12}B	1.2	0.44	0.15	0.59	25
	1.9	0.38	0.31	0.69	45
	2.5	0.29	0.63	0.92	68

critical excitation energy obtained from the analysis of the caloric curves by Natovitz *et al.* is presented in Fig. 7 together with critical energies found from p+Al collisions investigated in the present work. The former results were averaged in Ref. 7 over thirty units of mass of decaying nuclei and were attributed to the central value of each mass region. The present results correspond to multifragmentation of an ensemble of excited nuclei with the average mass $\langle A \rangle = 18.7$ and with the standard deviation of masses $\sigma(A) = 2.6$. It is clear that the present values of the critical excitation energy fit perfectly to the compilation of data obtained from the study of caloric curves. The values of the critical energies from

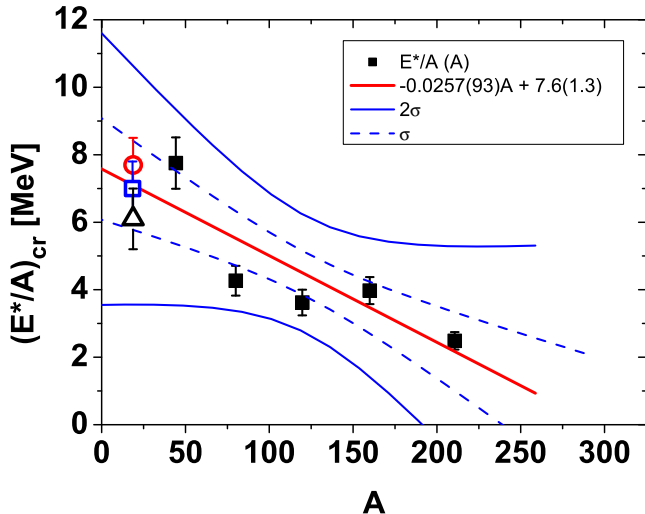


FIG. 7: The full squares represent the compilation of critical excitation energies per nucleon as a function of mass number of decaying nuclei obtained from the study of caloric curves [24], the solid straight line shows the linear regression of these data whereas the dashed and solid hyperbolas correspond to one- and two- standard deviation confidence intervals of the regression line, respectively. The empty symbols depict the critical excitation energy values used in the present analysis for p+Al collisions; circle, square, and triangle correspond to 1.2, 1.9, and 2.5 GeV beam energy, respectively.

the present study lay for all three proton beam energies inside the confidence interval of one standard deviation around the regression line approximating the mass dependence of the critical energy per nucleon.

IV. SUMMARY

In the present work the hypothesis was investigated, claiming that the energy and angular distributions of the double differential cross sections $d^2\sigma/d\Omega dE$ for intermediate mass fragments from inclusive measurements of reactions proceeding in the p+Al system at GeV proton beam energies can be reproduced by a reaction model in which a specific two-step mechanism is involved. In the first stage of the reaction a cascade of nucleon-nucleon and pion-nucleon collisions appears leaving an ensemble of the excited residual nuclei. These nuclei decay in the next stage of the reaction according to two competing scenarios: (i) The nuclei with the excitation energy per nucleon smaller than some critical value $(E^*/A)_{cr}$ - treated as a parameter, decay by a sequential emission of evaporated particles, (ii) the nuclei excited to energies above the limiting value $(E^*/A)_{cr}$ are subjects to multifragmentation. The first of these mechanisms is responsible for populating the low energy part of the spectra, whereas the second leads to emission of also higher energy intermediate mass fragments.

The excellent agreement of the calculated within such a model differential cross sections $d^2\sigma/d\Omega dE$ with the experimental data confirms the validity of the assumed hypothesis.

The investigations performed in the present work provide also the following conclusions:

- It was found that all intermediate mass fragments are products of the second stage of the reaction with a relative contribution of multifragmentation of the remnants of the nucleon-nucleon cascade systematically increasing with the proton beam energy.
- The only free parameter of the calculations mentioned above was the critical excitation energy $(E^*/A)_{cr}$ which decides which option of the decay of the excited remnants of the nucleon-nucleon cascade should be chosen. The second parameter which could in principle vary, *i.e.* the reduced freeze-out radius r_0 , appeared to be independent of the beam energy and to be equal to 1.4 fm, *i.e.* to the default value used in the Fermi breakup model (see *e.g.* ref. [23]).
- The value of the critical energy found from the present analysis of the inclusive spectra is compatible with those obtained from the study of the caloric curves. Therefore, it may be concluded that the investigation of intermediate mass fragment spectra obtained in inclusive measurements may be used as an alternative method to studying of the caloric curves for the extraction of the critical excitation energy per nucleon.

Successful description of the intermediate mass fragment emission from p+Al collisions in the 1.2 - 2.5 GeV proton beam energy range suggests that a similar picture of the reaction mechanism might be also appropriate for heavier nuclear systems as, *e.g.*, p+Ni or p+Au where another model of the IMF emission has been proposed [1–4].

Acknowledgments

The technical support of A.Heczko, W. Migdał, and N. Paul in preparation of experimental apparatus is greatly appreciated. This work was supported by the European Commission through European Community-Research Infrastructure Activity under FP6 project Hadron Physics (contract number RII3-CT-2004-506078), and Hadron-Physics2 (contract number 227431). One of us (M.F.)

acknowledges gratefully financial support of Polish Ministry of Science and Higher Education (Grant No N N202

174735, contract number 1747/B/H03/2008/35).

-
- [1] A. Bubak, A. Budzanowski, D. Filges, F. Goldenbaum, A. Heczko, H. Hodde, L. Jarczyk, B. Kamys, M. Kistryn, St. Kistryn, St. Kliczewski, A. Kowalczyk, E. Kozik, P. Kulessa, H. Machner, A. Magiera, W. Migdał, N. Paul, B. Piskor-Ignatowicz, M. Puchała, K. Pysz, Z. Rudy, R. Siudak, M. Wojciechowski, and P. Wüstner, *Phys. Rev. C* **76**, 014618 (2007)
- [2] A. Budzanowski, M. Fidelus, D. Filges, F. Goldenbaum, H. Hodde, L. Jarczyk, B. Kamys, M. Kistryn, St. Kistryn, St. Kliczewski, A. Kowalczyk, E. Kozik, P. Kulessa, H. Machner, A. Magiera, B. Piskor-Ignatowicz, K. Pysz, Z. Rudy, R. Siudak, and M. Wojciechowski, *Phys. Rev. C* **78**, 024603 (2008)
- [3] A. Budzanowski, M. Fidelus, D. Filges, F. Goldenbaum, H. Hodde, L. Jarczyk, B. Kamys, M. Kistryn, St. Kistryn, St. Kliczewski, A. Kowalczyk, E. Kozik, P. Kulessa, H. Machner, A. Magiera, B. Piskor-Ignatowicz, K. Pysz, Z. Rudy, R. Siudak, and M. Wojciechowski, *Phys. Rev. C* **80**, 054604 (2009)
- [4] A. Budzanowski, M. Fidelus, D. Filges, F. Goldenbaum, H. Hodde, L. Jarczyk, B. Kamys, M. Kistryn, St. Kistryn, St. Kliczewski, A. Kowalczyk, E. Kozik, P. Kulessa, H. Machner, A. Magiera, B. Piskor-Ignatowicz, K. Pysz, Z. Rudy, R. Siudak, and M. Wojciechowski, *Phys. Rev. C* **82**, 034605 (2010)
- [5] R.E.L. Green, R.G. Korteling, *Phys. Rev. C* **22**, 1594 (1980)
- [6] R.E.L. Green, R.G. Korteling, J.M. DAuria, K.P. Jackson, R.L. Helmer, *Phys. Rev. C* **35**, 1341 (1987)
- [7] C.-M. Herbach, D. Hilscher, U. Jahnke, V.G. Tishchenko, J. Galin, A. Letourneau, A. Péghaire, D. Filges, F. Goldenbaum, L. Pieńkowski, W.U. Schröder, and J. Töke, *Nuclear Physics A* **765**, 425 (2006)
- [8] A. Letourneau, A. Böhm, J. Galin, B. Lott, A. Péghaire, M. Enke, C. M. Herbach, D. Hilscher, U. Jahnke, V. Tishchenko, *et al.*, *Nucl. Phys. A* **712**, 133 (2002)
- [9] G. D. Westfall, R. G. Sextro, A. M. Poskanzer, A. M. Zebelman, G. W. Butler, and E. K. Hyde, *Phys. Rev. C* **17**, 1368 (1978)
- [10] E.K. Hyde, G.W. Butler, A.M. Poskanzer, *Phys. Rev. C* **4**, 1759 (1971)
- [11] A.M. Poskanzer, G.W. Butler, E.K. Hyde, *Phys. Rev. C* **3**, 882 (1971)
- [12] J. Richert, P. Wagner, *Physics Reports* **350**, 1 (2001)
- [13] B. Borderie, M.F. Rivet, *Prog. Part. Nucl. Phys.* **61**, 551 (2008)
- [14] Z. Fraenkel, E. Piasetzky, G. Kalbermann, *Phys. Rev. C* **26**, 1618 (1982)
- [15] A. Bubak, B. Kamys, M. Kistryn, B. Piskor-Ignatowicz, *Nucl. Instr. Meth. in Phys. Research B* **226**, 507 (2004)
- [16] A. Boudard, J. Cugnon, S. Leray, and C. Volant, *Phys. Rev. C* **66**, 044615 (2002)
- [17] A. Boudard, J. Cugnon, S. Leray, and C. Volant, *Nucl. Phys. A* **740**, 195 (2004)
- [18] S. Furihata, *Nucl. Instr. and Meth. in Phys. Research B* **71**, 251 (2000)
- [19] S. Furihata and T. Nakamura, *Journal of Nuclear Science and Technology Supplement* **2**, 758 (2002)
- [20] A. Magiera, computer program ROZPAD (2010) - unpublished
- [21] E. Fermi, *Prog. Theor. Phys.* **5**, 1570 (1950)
- [22] A. Gökmen, G. J. Mathews, V. E. Viola, Jr., *Phys. Rev. C* **29**, 1606 (1984)
- [23] <http://geant4.web.cern.ch/geant4/support/userdocuments.shtml> (Geant4 Physics Manual)
- [24] J. B. Natowitz, R. Wada, K. Hagel, T. Keutgen, M. Murray, A. Makeev, L. Qin, P. Smith, and C. Hamilton, *Phys. Rev. C* **65**, 034618 (2002)